

# Corn Yield Prediction Model with Deep Neural Networks for Smallholder Farmer Decision Support System

**Chollette Olisah<sup>1\*</sup>, Lyndon Smith<sup>1</sup>, Melvyn Smith<sup>1</sup>, Lawrence Morolake<sup>2</sup>, Osi Ojukwu<sup>3</sup>**

<sup>1</sup>Department of Engineering Design and Mathematics, University of the West of England, United Kingdom.

<sup>2</sup>Department of Computer Science, Baze Univeristy, Abuja, Nigeria.

<sup>3</sup>Morph Innovations Limited, Lagos, Abuja, Nigeria.

**\* Correspondence:**

[chollette.olisah@uwe.ac.uk](mailto:chollette.olisah@uwe.ac.uk), UWE Bristol - Frenchay Campus, Coldharbour Ln, Bristol BS16 1QY

## **Abstract**

Crop yield prediction has been modeled on the assumption that there is no interaction between weather and soil variables. However, this paper argues that an interaction exists, and it can be finely modelled using Kendall Correlation coefficient. Given the nonlinearity of the interaction between weather and soil variables, a novel deep neural network regressor (DNNR) was carefully designed with considerations to the depth, number of neurons of the hidden layers, and the hyperparameters with their optimizations. Additionally, a new metric, the average of absolute root squared error (ARSE) was proposed to address the shortcomings of root mean square error (RMSE) and mean absolute error (MAE) while combining their strengths. Using the ARSE metric, the random forest regressor (RFR) and the extreme gradient boosting regressor (XGBR), were compared with DNNR. The RFR and XGBR achieved yield errors of 0.0000294 t/ha, and 0.000792 t/ha, respectively, compared to the DNNR(s) which achieved 0.0146 t/ha and 0.0209 t/ha, respectively. All errors were impressively small. However, with changes to the explanatory variables to ensure generalizability to unforeseen data, DNNR(s) performed best. The unforeseen data, different from unseen data, is coined to represent sudden and unexplainable change to weather and soil variables due to climate change. Further analysis reveals that a strong interaction does exist between weather and soil variables. Using precipitation and silt, which are strong-negatively and strong-positively correlated with yield, respectively, yield was observed to increase when precipitation was reduced and silt increased, and vice-versa. Although the degree of decrease or increase was not quantified in this paper. Contrary to existing yield models targeted towards agricultural policies and global food security, the goal of the proposed corn yield model is to empower the smallholder farmer to farm smartly and intelligently through a designed mobile application decision support system with educative module, and farmer-to-market access module.

**Keywords:** corn yield prediction, deep neural networks, machine learning, decision support system, smallholder farmer

## 1 Introduction

The role of the smallholder farmer is critical to global food security. In Sub-Saharan Africa, the smallholder farmer constitutes about 80% of crop farmers [1], and yet the region is challenged with an acute food insecurity crisis. As highlighted in the 2022 Global Report on Food Crises (GRFC) mid-year update, around 140 million people in Sub-Saharan Africa are experiencing severe food insecurity. Several factors can impact smallholder food production capacities, which are summarized in this paper as secondary and primary factors, based on the level of effect on the food production capacities of the smallholder farmer. The secondary-level factors result from the impact of agricultural and rural policies [2], and weather variability [3] on food production capacities and cannot be directly controlled by the smallholder farmer. The primary-level factors, on the other hand, can be directly controlled by the farmer; examples are lack of access to the market, poor education, and lack of technology for precision farming [4]. This paper argues that when technology is leveraged, the smallholder farmer can overcome the challenges of the primary-level factors, which could potentially increase food production and impact food security in Africa.

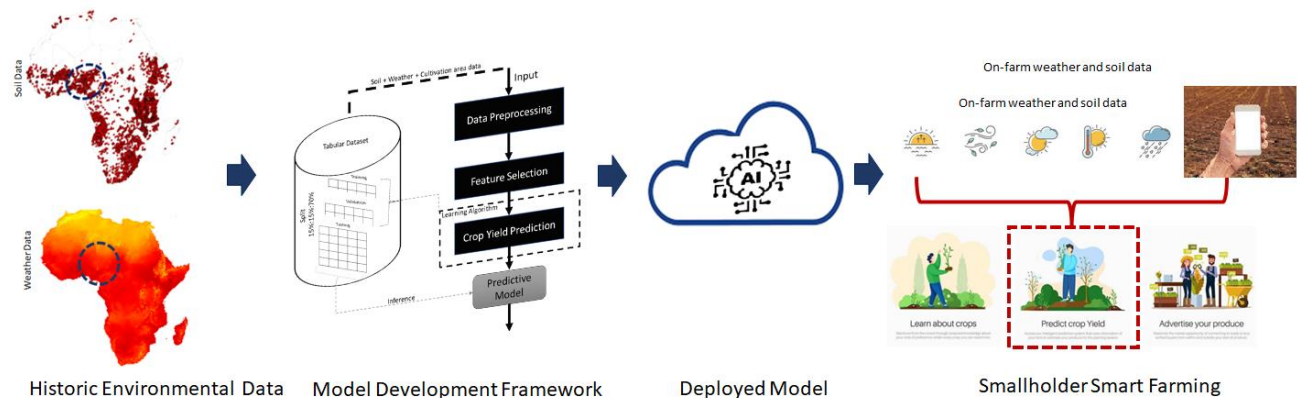
Technology in the form of robots [5], sensors [6], drones [7], and decision systems [8] – [16] are currently enabling radical transformations in precision agriculture. Aside from a decision system that can be designed with inexpensive predictive models, other technologies are costly and might be out of the reach of the smallholder farmer. As a result, subsequent discussions will review ways decision systems have been explored in literature for smart farming.

The decision systems are approached in the existing literature from the perspective of crop yield prediction that is aimed at helping governments to monitor food production, improve agriculture policies, and monitor food security. Jeong et al. [11] trained the random forest (RF) machine learning algorithm for crop yield prediction. Alhnaity et al. [12] applied long short-term memory (LSTM) for predicting tomato yield in a controlled environment. Using 142,952 samples of maize data comprising plant genotypes, weather, and soil variables, [13] designed a deep neural network (DNN) algorithm for yield prediction. Their DNN architecture comprised 21 hidden layers with 50 neurons in each layer. In [14] two convolutional neural networks (CNN), which they termed weather CNN (W-CNN) and soil CNN (S-CNN), were designed for modelling temporal and spatial information on weather and soil data. The spatial information was retrieved from the fully connected (FC) layer of W-CNN and S-CNN. The spatial data, along with the temporal data, historic yield, and management data, were fed to a recurrent neural network (RNN) for forecasting yield. Similarly, Shahhosseini et al. [15] used a W-CNN and S-CNN to model weather and soil, while a DNN was used for the management data. These models

were used to construct a homogeneous ensemble model for corn yield prediction. In [16] an ensemble machine learning model was created by combining the following: linear regression, least absolute shrinkage, and selection operator (LASSO) regression, extreme gradient boosting (XGBoost), light gradient boosted machine (lightGBM), and RF for predicting corn yield.

Aside from the fact that existing work approaches crop yield prediction in a way that benefits the government and commercial farms more than the smallholder farmer, some of the work in the design of yield predictive models [14]-[16], appears to have assumed that the environmental variables such as soil and weather are independent of each other. However, the interaction between climate and soil is an integral part of plant growth [17], [18]. Additionally, there is no existing tool that overcomes the primary-level challenges such as farmer education, access to the market, and predictive models, that directly impact the smallholder farmer. Therefore, this paper proposes a decision support system (see Figure 1) for the smallholder farmer with contributions summarized as follows: 1) a novel preprocessing pipeline to address the challenges observed with the real-world collected crop yield data, 2) design of a novel deep convolutional neural network model which learns the dynamic interactions between soil, weather, and farm geographical location for crop yield prediction, 3) a new regression metric that combines RMSE and MAE to address their shortcomings while utilizing their strengths, and 4) a mobile application decision support system that integrates the proposed predictive model(s) with inclusion of modules to aid with farmer education, and market access. The proposed decision support system provides smallholder farmers with inexpensive ways to farm smart via a smartphone that is readily available to them, while utilizing locally sourced information on the farm to make informed decisions for their farmland for a planting season. This paper only focuses on single time step yield for the corn plant. The remaining parts of the paper are structured as follows: Section 2 describes the research methodology, and section 3 presents the experimental settings, results, and discussions. Then finally, in section 4, the conclusion summarizes the findings of the paper.

**Fig. 1**

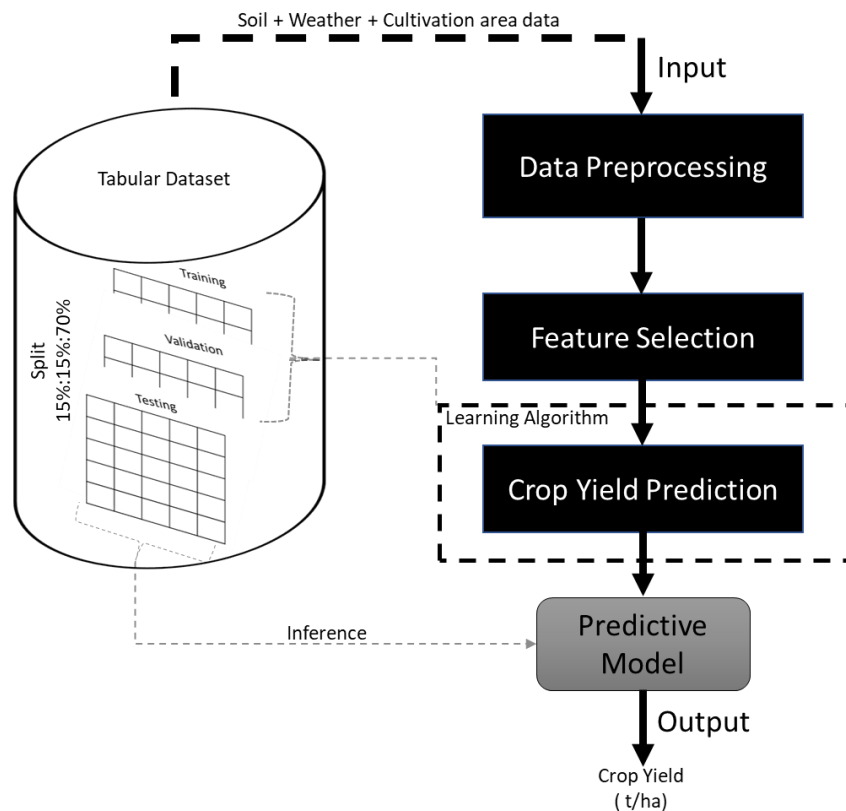


The architecture of proposed crop yield system

## 2 Methodology

The proposed methods are presented and discussed under the following headings: data preprocessing, feature selection, and crop yield prediction, and the pipeline is depicted in Figure 2. The process begins with the collection of raw climate, weather, and environment data for Africa with Nigeria as the reference region. Then proceeds to preprocessing the data to prepare it for corn yield prediction that is useful to a smallholder farmer, and then the interaction between the data is analyzed using a statistical correlation technique, to identify the explanatory variables that contribute most significantly to the outcome variable, corn yield. The selected variables/features then make up the dataset, which was split to obtain sets for training the prediction algorithms for building an efficient predictive model to be used for inferencing. During inferencing the predictive model is applied to a data point, usually from the test set, (i.e. unseen during training) to predict the outcome variable, corn yield. This is to ensure that the performance of the prediction model is not overfitting to the training (seen) set but can generalize to unseen data.

**Fig. 2**



The proposed corn yield prediction architecture

## 2.1 Study Region and Data Collection

As a reference study region in Africa, Nigeria was selected because there are over 211.4 million people, of which a large percentage of the population are smallholder farmers [19] who are mostly corn growers. Nigeria [9.0820° N, 8.6753° E] has an arable land area of 34 million hectares [19], is located on the west coast of Africa and comprises 36 states having 214 and 10 as the most and least number of districts, respectively. For each state, the environmental data were collected as follows.

- i. Grid map climate data which comprised eight (8) climate variables, namely: average temperature  $C^0$ , minimum temperature  $C^0$ , maximum temperature  $C^0$ , precipitation ( $mm$ ), solar radiation ( $kJ\ m^{-2}\ day^{-1}$ ), wind speed ( $m\ s^{-1}$ ), and water vapor ( $kPa$ ) taken at 30 seconds (s), 2.5 minutes (m), 5 m, and 10 m spatial resolutions from  $\sim 1\ km^2$  to  $\sim 340\ km^2$  were obtained from the high spatial resolution WorldClim [20] global climate database. The data per grid point on the map is monthly climate data from January to December of each year between 1970 and 2000.
- ii. The yearly corn yield was computed for 1000 *metric tonnes* for a 1000 *hectares* cultivation area and spans from 1995 to 2006. These data were obtained from a data repository owned by Kneoma Corporation [21].
- iii. Grid map soil data of 250 minutes spatial resolution were retrieved from AfSIS [22]. It includes wet soil bulk density, dry bulk density ( $kg\ dm^{-3}$ ), clay percentage of plant available water content, hydraulic conductivity, the upper limit of plant available water content, the lower limit of, organic matter percentage, pH, sand percentage ( $g\ 100\ g^{-1}$ ), silt percentage ( $g\ 100\ g^{-1}$ ) and, clay percentage ( $g\ 100\ g^{-1}$ ), and saturated volumetric water content variables measured at depths 0–5, 5–10, 10–15, 15–30, 30–45, 45–60, 60–80, 80–100, and 100–120 measured in centimeters (cm). The soil data span is from 1960 to 2012.
- iv. The Geolocation coordinates (latitude and longitude) of each state were obtained from Google Maps. Then used to extract the point values from the grid maps of each environmental variable (climate and soil) at specific district locations of the 36 states in Nigeria using the Esri-ArcGIS professional 2.5 software tool.

## 2.2 Data Preprocessing

The environmental data: climate, soil, cultivation area, and crop yield data required some levels of preprocessing. The reasons are as follows: 1) inconsistent year intervals of the environmental data because they were acquired from different sources. The crop yield data, and soil data covered periods between 1995 to 2006, and 1960 to 2012, respectively, 2) some weather and soil variables might not be available to a smallholder farmer, and 3) missing data - weather, soil or cultivation area data showed missing data for some districts of a state and in some cases, the entire state. Given below are preprocessing approaches applied to the data to prepare it for learning.

- i. Aggregate weather and soil data across resolutions. Using the monthly weather data across the spatial resolutions of 30 s, 2.5 m, 5 m, and 10 m, compute the average of all climate data. Likewise, aggregate the soil data across depths 0–5, 5–10, 10–15, 15–30, 30–45, 45–60, 60–80, 80–100, and 100–120 in centimeters (cm).
- ii. Forecast the yearly crop yield data in tonnes per hectare and cultivation area in hectares in 6-time steps, that is, from 2006 to 2012, so it closely matches the soil data. This is on the assumption that weather variables might be inversely related to yield, while soil variables are more likely to be directly related to yield. To achieve this goal, the autoregressive integrated moving average (ARIMA) [23] was used. Then were averaged into a single value for a state.
- iii. Merge the climate, soil, yield, and cultivation area data into a single set. This step helped to reveal the states or districts with missing values. After the missing values were removed, the number of states reduced from 36 to 23 and are they are: Abia, Abuja, Akwa Ibom Anambra, Bayelsa, Benue, Cross river, Delta, Ebonyi, Edo, Ekiti, Enugu, Imo, Kebbi, Kwara, Lagos, Ogun, Ondo, Osun, Oyo, Plateau, Rivers, Taraba. Then, only retain environmental variables that can easily be accessible to the smallholder farmer comprise [24] – [26].
- iv. Average the yield and hectare data across years, then transform them to values realistically achievable by a smallholder farmer. The transformation functions are mathematically expressed as given in eq. (1) and eq. (2), respectively.
- v. Using Kendall correlation coefficient, identify the environmental variables that significantly interact with yield.

$$Y'_i = \left(\frac{Y_i}{O_t}\right) * \frac{E_h}{E_y} \quad i = 0, 1, 2, \dots, N \quad (1)$$

$$H'_i = \left(\frac{H_i}{O_h}\right) * E_h \quad (2)$$

where  $Y_i$  and  $H_i$  are the yield and hectare values per state,  $Y_{max}$  and  $H_{max}$  the maximum expected yield<sup>1</sup> and hectare<sup>2</sup> values for smallholders in the region, number of metric tonnes yield was originally measured in per state,  $O_h$  and size of the cultivation area in hectares the yield was originally measured in per state,  $O_t$ .

### 2.2.1 Forecasting

ARIMA [23] is a simple statistical technique for solving non-seasonal and patterned time series prediction problems. It combines auto-regressive (AR) and moving average (MA) models for forecasting future timesteps using historic observations and random errors. ARIMA is characterized by three terms: AR order term,  $p$ , which signifies the number of prior values to be used as predictors in the model, AR series stationary parameter  $d$ , and

<sup>1</sup> [https://www.fao.org/fileadmin/templates/nr/sustainability\\_pathways/docs/Factsheet\\_SMALLHOLDERS.pdf](https://www.fao.org/fileadmin/templates/nr/sustainability_pathways/docs/Factsheet_SMALLHOLDERS.pdf)

<sup>2</sup> <https://knoema.com/atlas/Nigeria/topics/Agriculture/Crops-Production-Yield/Maize-yield>.

MA order term,  $q$ , which indicates the number of forecast errors of past values. This is required by the ARIMA Model to forecast future points in the series. The AR and MA models are then combined to form an ARIMA model [23]. This process is mathematically given as follows.

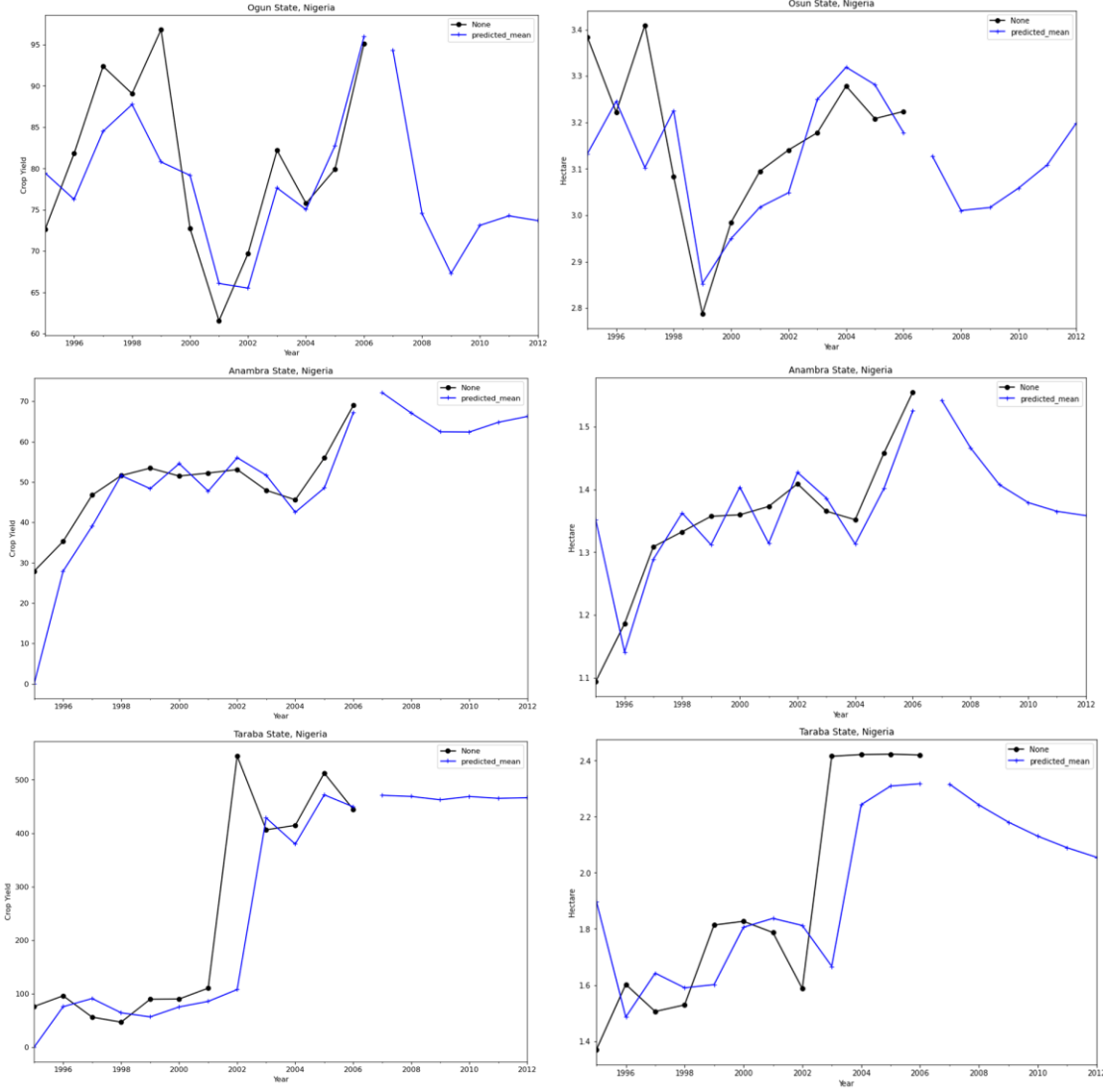
$$\hat{Y}_t = \alpha + \beta_1 Y_{t-1} + \beta_2 Y_{t-2} + \cdots + \beta_p Y_{t-p} + \epsilon_t + \phi_1 \epsilon_{t-1} + \phi_2 \epsilon_{t-2} + \cdots + \phi_q \epsilon_{t-q} \quad (3)$$

where  $\alpha$  is a constant,  $\epsilon_t$  is the error term at time  $t$ ,  $\beta_1, \beta_2, \beta_3, \dots, \beta_p$  are the AR parameters, and  $\phi_1, \phi_2, \phi_3, \dots, \phi_q$  are the MA parameters and are combined to form  $\hat{Y}_t$ , the future points in the series.

Typically, to predict future data points of a time series data using the ARIMA model, the stationarity of the series data will have to be tested using the augmented Dickey Fuller (ADF) [27] test. The null hypothesis of the ADF test by default represents the non-stationarity of the series, but if the p-value of ADF test is less than the significance level ( $p=0.05$ ) then the series is considered stationary. If the series passes the ADF test and is considered stationary, then the values of  $p$  and  $q$  terms can be determined by observing  $p$ -values above the significance level,  $p=0.05$  for the autocorrelation function and partial autocorrelation plots [27], respectively.

The crop yield and cultivation area data are extended by six (6) time steps to closely match in years to the soil data. The outcome of forecasting for some states is shown in Figure 3. This step depends on the outcome of ADF test, partial autocorrelation, and autocorrelation functions. The importance of the ADF test is demonstrated using the following example: the yield and cultivation area for Ogun, Anambra, and Taraba states with their  $p$ ,  $d$ ,  $q$  terms given as (5,0,1; 5,0,1), (2,1,1; 1,0,1), and (2,1,1;10,1). Their p-values are (0.000000; 0.000000), (0.343881; 0.997572), and (0.450462, 0.859081), respectively. Based on the significance test using the p-values, Ogun state series is considered a stationary series. However, Anambra and Taraba states are considered non-stationary series. Therefore, they will require differencing to convert them to stationary series. It should be noted that the cultivation area data was normalized by logarithmic transformation before forecasting with ARIMA because it was highly skewed and afterwards was reversed.

**Fig. 3**



Forecasting future timesteps of historic yield and cultivation area in hectare using ARIMA. This is repeated for all the 36 states of Nigeria. However, only the results of forecasting achieved for 3 states, Anambra, Osun, and Taraba states are visualized.

### 2.3 Feature Selection

Feature selection is a key step in machine learning (ML) for identifying intrinsic features in a dataset. This prevents ML models from overfitting to noise and generalizing to unseen data. To select significant features, the Kendall Correlation [28] method was employed. Kendall correlation is a non-parametric statistical correlation technique that measures the strength of association between two variables. This functionality makes Kendall correlation a useful tool for describing the interaction between crop yield,  $y$ , and any of the environment variables,  $x$ .

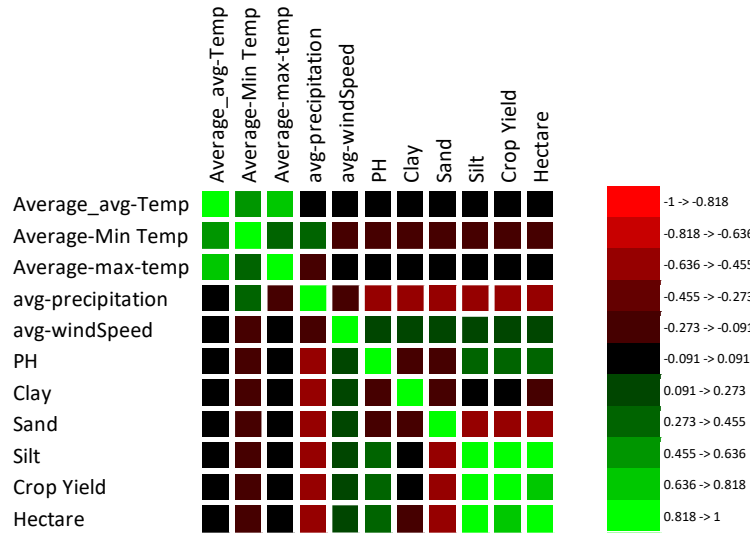
$$\tau_{x,y} = P(\sum_{i < j} \text{sgn}(x_i - x_j) \cdot \text{sgn}(y_i - y_j)) \quad (4)$$



where  $n$  is the size of the variables  $(x, y)$  under observation which do not necessarily need to be ranked or ordered [29] and  $P$  is the total number of possible pairings of  $x$  with  $y$  observations given as  $2/n \cdot (n - 1)$ , and  $sgn()$  returns the sign of a real number.

The strength of the association between two variables is given by the Kendall's coefficient  $\tau_{x,y}$ , which range between values of  $-1$  and  $+1$ , for perfect negative and positive correlation, respectively. These coefficients are coded as color maps in the correlation plot presented in Figure 4. A value  $> 0$  shows a positive relationship where both the explanatory and outcome variables increase together, whereas with a value  $< 0$ , an increase in one will result in the decrease of the other. A value of  $0$  indicates that no relationship exists between both variables. The Kendall correlation amongst other statistical tools was used because the dataset is skewed and contains relevant outliers (see Figure 5). With exclusion of the state variable, which is a categorical variable, the Kendall correlation was applied to the numeric features using the XLSTAT statistical 2020 software. The correlation coefficients obtained for average temperature, average minimum temperature, average maximum temperature, average precipitation, average wind speed, pH, clay, sand, silt, crop yield, and hectare, are  $-0.080$ ,  $-0.208$ ,  $-0.073$ ,  $-0.475$ ,  $0.191$ ,  $0.329$ ,  $-0.046$ ,  $-0.560$ ,  $1.000$ ,  $1$ , and  $0.727$ , respectively.

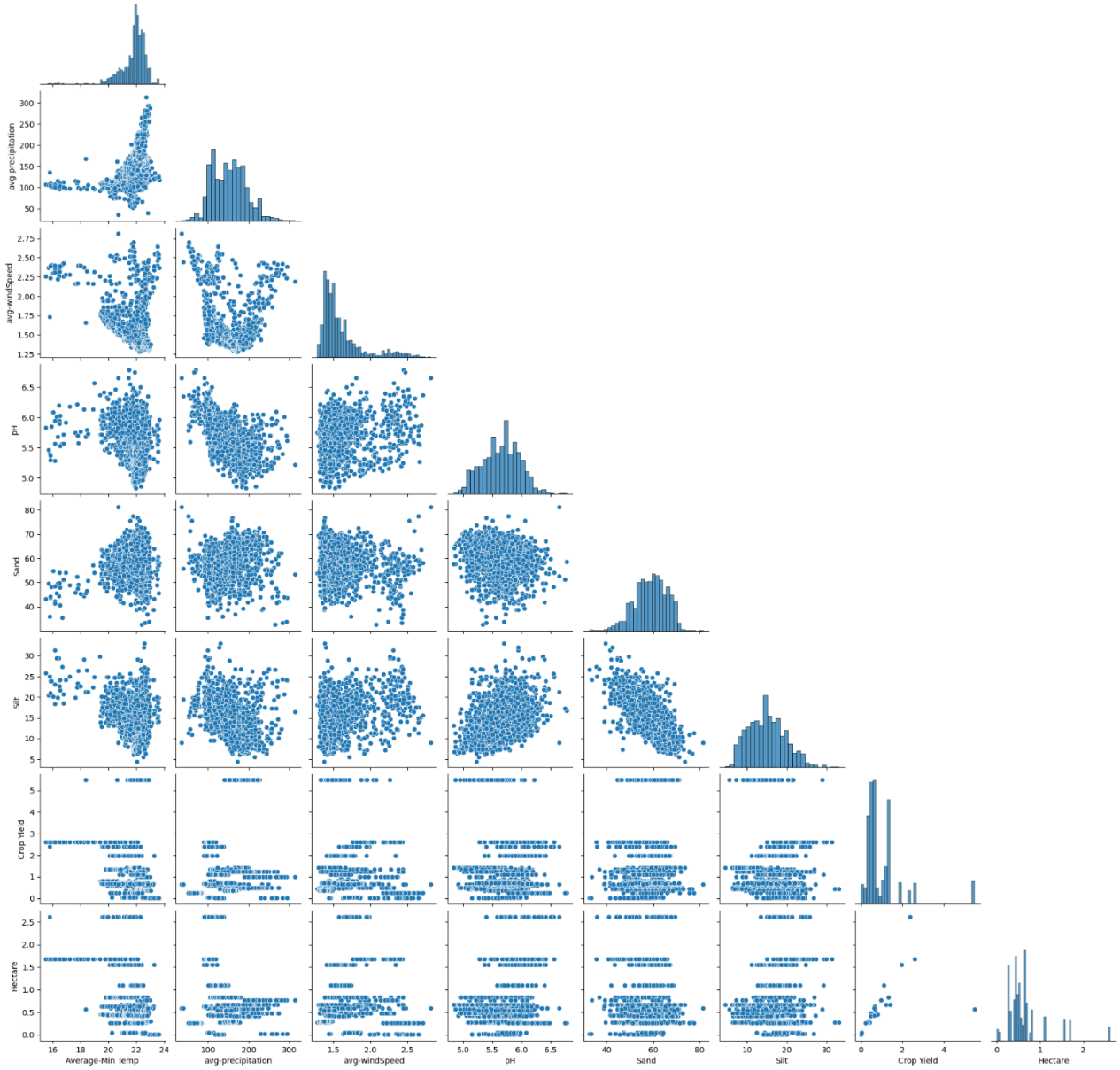
**Fig. 4**



The Kendall correlation coefficient for measuring the strength of association between the explanatory variables and outcome variables. The further the Kendall coefficient of an explanatory variable deviates from  $0$ , the higher its association to the outcome variable, with  $0$  indicating no association. The correlation coefficients of hectare (cultivation area), silt, average precipitation, sand, soil pH, wind speed, and average minimum temperature, (organized in the other of importance) show to be more

associated to yield. The results show that silt and hectare explanatory variables are more highly correlated to yield.

**Fig. 5**



Scatter plot visualization of the data distribution. Most of the explanatory variables can be observed to show nonlinear association to the outcome variable.

## 2.4 Crop Yield Prediction

Since the goal is to design a decision support system that maximizes efficiency by employing the predictive power of machine learning, the deep neural network (DNN), XGBoost, and RF, which are well known to achieve high-performance accuracies on small sample tabular data are explored for the regression task of crop yield

prediction. The DNN architecture and hyperparameters were designed by taking into consideration the data size, its complexity, and experimental variables while XGBoost and RF were designed through hyperparameter optimization. Though these algorithms are popularly applied to classification tasks, they were utilized for this paper's regression task and will henceforth be renamed, deep neural network regressor (DNNR), extreme gradient boosting regressor (XGBoostR), and random forest regressor (RFR).

#### 2.4.1 Deep Neural Network Regressor

The DNN is structured based on a feed-forward architecture that passes each neuron from the input layer, with associated weights and bias after transformation by nonlinear activation, to the hidden layer. Then, from several hidden layers and activation functions, a decision can be reached at the output layer. This process is repeated using the backpropagation algorithm as presented in [30] for weight update of the neuron until the error function is minimized. The neuron activation at the hidden layer and weight update through backpropagation are expressed as:

$$f(x) = \varphi(\sum_i^n w_i x_i + b) \quad (5)$$

where the function,  $f$ , outputs a decision for an input neuron  $x_i$ , which is either to pass the neuron from one hidden layer to the next or not. This decision is obtained through a weighted sum of neurons,  $x_i$  and weight  $w_i$  with added bias,  $b$ , and it is mapped to a desired range using the activation function,  $\varphi$ .

The hidden layer is the powerhouse of a DNN algorithm because the depth and number of neurons of the layer amongst other hyperparameters determine the capability of the network to address the complexity of the problem solved. The more complex the problem, the deeper the depth of the hidden layer, and vice versa. Also, with tabular data, the number of neurons can be determined from the number of variables and the size of the data. It has been shown in [31] that when the number of neurons is set to twice the number of variables in tabular data, the network begins to learn the intrinsic information of the data. The same concept was adopted in this paper; however, it was approached with a twist to how it transcends through the hidden layers. Since the complexity cannot be easily determined by the nonlinearity of the data and the number of variables, the grid search method is relied on for choosing the optimal depth of the hidden layers and other hyperparameters. In all, the proposed DNNR architecture (see Figure 6) was designed as follows: input layer - 30 neurons, hidden layer - 3 and 64 for the depth and number of neurons per layer, and output layer - a single numeric value that represents crop yield. The hyperparameters are rectified linear unit (ReLU) activation function [32] which is applied to Eq. 5 and has been shown in literature to be best used for overcoming the vanishing gradient problem of a network. The learning rate was set to 0.001 using the Adam optimizer which controls the weight update of the network. Epoch was set to 60 to enable the network to make 60 passes through the entire training set, in a batch size of 100,

during which weight update to a neuron is made 12 times. The loss function used during weight update (backpropagation) was the mean absolute error (MAE) which is expressed as:

$$L(\emptyset) = \frac{1}{B} \sum_{i=1}^B |y_i - \hat{y}_i| \quad (6)$$

where  $L$  is the objective function with error determined by computing the difference between  $\hat{y}_i$ , the predicted and  $y_i$ , the true value, and  $B$  is the total number of data points in each batch. The error value becomes input to the backpropagation computation process, given as:

$$w_x^* = w_x - \left( r * \left( \frac{\partial Error}{\partial w_x} \right) \right) \quad (7)$$

where the first term includes the weight of an input neuron  $w_x$ , and the last term includes the partial derivative of the error function  $\left( \frac{\partial Error}{\partial w_x} \right)$  multiplied with the learning rate,  $r$ . By subtracting the first term from the second term, the weight for a given input neuron can be updated.

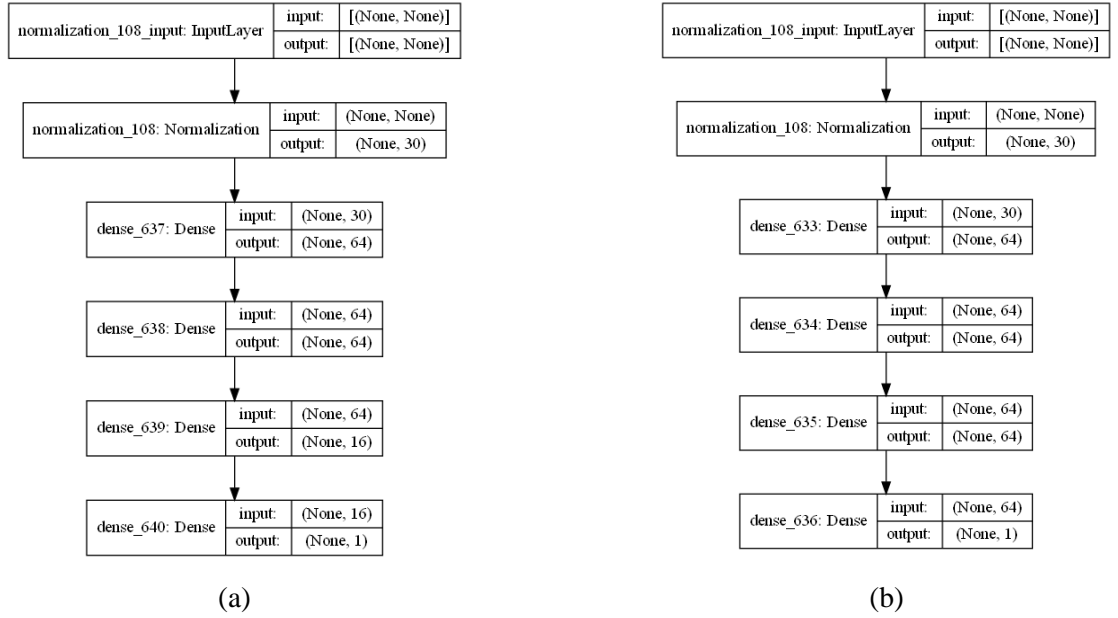


**Figure 6** The architectures of the DNNs. The architecture for DNN16 (a) and DNN64 (b) both include a data normalization layer.

#### 2.4.2 Extreme Gradient Boosting Regressor

XGBoost [33] is developed based on the concept of the gradient boosting decision tree (GBDT) algorithm [34]. It builds multiple decision trees that are organized in sequences such that a preceding tree error helps towards

minimizing the prediction error of subsequent trees. In this way, a strong model of decision trees is formed. XGBoost advances this functionality by introducing the L1 and L2 regularizers to stabilize the generalization capability of GBDT. This is expressed mathematically as:

$$L(\phi) = \sum_{i=0}^n l(\hat{y}_i, y_i) + \sum_{k=0}^n \Omega(f_k) \quad (8)$$

where the objective of function,  $L(\phi)$  is to impose a penalty on erroneous predictions in order to minimize the error of the model by adding a regularization function,  $\Omega(f_k)$  to the loss function  $l(\hat{y}_i, y_i)$  computed between the model's predicted value,  $\hat{y}_i$ , and actual value,  $y_i$ .

To predict a continuous numeric value, the negative mean average error loss function is used, thus XGBoost is referred to as XGBR. Modification to the XGBR is via hyperparameter optimization with values of the hyperparameters determined through the grid search method. For explicit discussions on the concept of the grid search method and how it is used in this paper, the reader is referred to [31]. Through grid search, the number of estimators, number of trees, maximum depth, learning rate, and minimum samples split XGBR hyperparameters were set as described in Table 1.

Table 1 Decision tree-based models hyperparameters and values.

Hyperparameter	Description	Model Values	
		XGBR	RFR
Number of estimators	Number of trees created from the training data	900	10
Maximum depth	Controls how specialized each tree is to the training data. The higher the value the more likely overfitting will occur.	10	10
Learning rate	Controls the pace at which new trees can make corrections to the error of previous trees.	0.1	
Minimum samples split	Specifies the minimum number of samples required at a leaf node for splitting to occur.	0.1	
Subsample	Signifies the number of training samples XGBoost uses to grow the trees.	1	

#### 2.4.3 Random Forest Regressor

RF is an ensemble of several decision trees [35] built through random sampling of training data. It uses the concept of bagging and feature randomness to ensure the decision trees at each time are presented with unique

samples of the training data. In this way, variance can be decreased without an increase in bias. For the regression task, the mean average error loss function was used to predict a continuous numeric value. Therefore, RF becomes a random forest regressor (RFR) and prediction from all individual trees generated from the random sample of the data,  $x$ , gets averaged over all trees  $t_i$ . The process is expressed mathematically as:

$$\hat{t} = \frac{1}{N} \sum_{i=1}^N t_i(x) \quad (9)$$

where  $x$  is the training data and  $N$  is the number of sets randomly created the dataset through bagging.

The RFR was optimized for the given task via the grid search method for selecting the optimal values of the following hyperparameters: number of estimators, maximum depth, minimum sample split, and minimum samples leaf.

### 3 Experiments, Results and Discussions

#### 3.1 Experimental Settings

The data used in this paper comprises explanatory and outcome variables. The explanatory variables are the average minimum temperature, average precipitation, average wind speed, soil pH, soil sand content, soil silt content, and cultivation area in hectare and the crop yield is the outcome variable. The explanatory variable was extended to include the state variable, which is a categorical datatype, but was converted to a numerical datatype through one-hot encoding. This further expanded the number of explanatory variables to 30 because there are 23 states retained after missing values were discarded. The inclusion of the state variable is to ensure that geolocation, which introduces changes in weather and soil composition, contributes to the decision of the predictive models. In all, the dataset comprised of 1827 data points and after missing values and duplicates were removed, only 1632 datapoints were retained. Then, after feature selection the data was split into training, validation and test sets with each set containing 1142, 245, and 245, data points, respectively. The data were further normalized for use by the DNNR based models.

Given that this paper solves a regression problem, the regression metrics suffice for the task. The RMSE is chosen so that performance of the corn yield predictive models from the viewpoint of sensitivity to outliers (RMSE) can be observed. Usually, if there exists a data point with large difference between the predicted and the actual, the RMSE error metric will capture it and record high errors. However, since the RMSE is sensitive to outliers, it becomes necessary to also introduce the MAE. The MAE has its own fair share of shortcomings, it is insensitive to outliers (MAE) and unable to reveal the presence of sample points with large disparity between the true value and predicted value. In this paper, both metrics are combined through averaging to utilize their benefits and overcome their shortcomings. The new metric is termed average of absolute root squared error (AARSE). These metrics are mathematically defined in Eq. (10-12).

To evaluate each predictive model's performance, the experiments will be presented and discussed under 1) the predictive models' overall performance with the training set, 2) predictive model performance using different evaluation metrics, 3) generalization capability of the predictive models, and 4) evaluation of significance of the feature selection step in the pipeline.

$$M_{RMSE} = \sqrt{\frac{1}{N} \sum_{i=1}^N (y'_i - y_i)^2} \quad (10)$$

$$M_{MAE} = \frac{1}{N} \sum_{i=1}^N |y'_i - y_i| \quad (11)$$

$$ARSE = \frac{1}{n} \sum_{i=1}^n (M_{RMSE}, M_{MAE}) \quad (12)$$

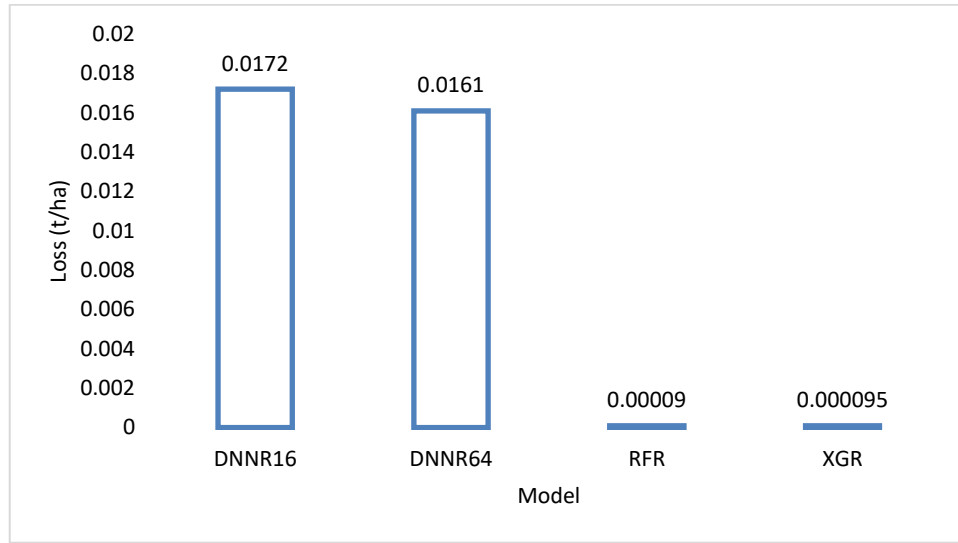
where  $N$  is the total number of test set data points,  $y'_i$  is the predicted and  $y_i$  is the true value,  $M_{RMSE}$  and  $M_{MAE}$  are the predicted errors for RMSE and MAE, and  $n$  is the number of errors.

## 3.2 Results

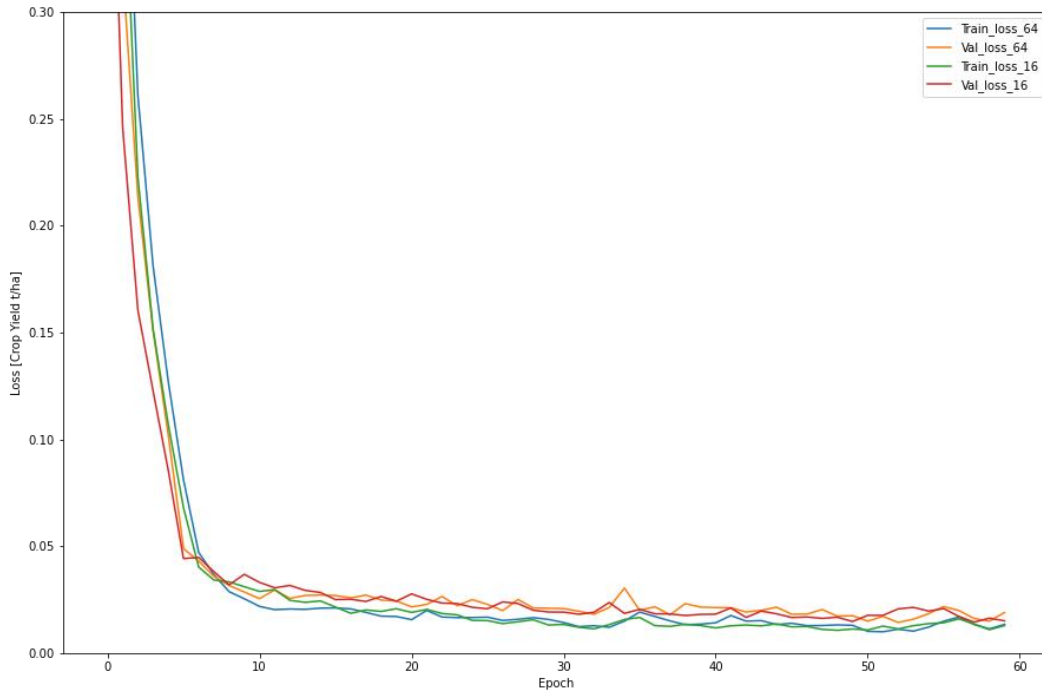
### 3.2.1 Performance of the Predictive Models on the Training Set

Since the crop yield prediction in this paper is focused on the smallholder farmer rather than commercial farms or Government monitoring of food production, improving agriculture policies, or monitoring food security, the corn yield prediction outputs a single-point prediction. This means that the farmer can use information such as soil pH, sand, and silt percentages, together with temperature, and precipitation. This data can be locally sourced from the farm to understand how productive the farmland is and can further improve it if it yields less than the farmer's estimation. Even though corn yield prediction has no associated risk like in clinical diagnosis, making an accurate decision is important to the farmer as any other risk related task. For this reason, the DNNR16, DNNR64, RFR, and XGBR predictive models were designed using the training set as a single set with results presented in Figure 7, and through 10-fold cross-validation with performance presented in Figure 8.

**Fig. 7**



(a)



(b)

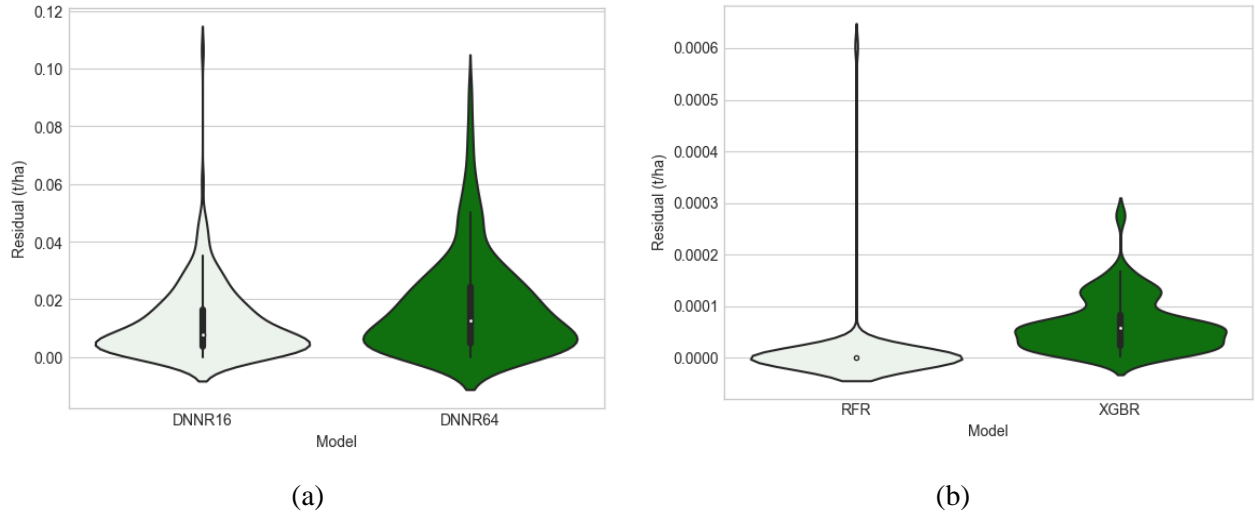
Visualizing performance on the training set. (a) the loss performance of the DNNR16, DNNR64, RFR, and XGBR models designed using training set as a single set. Training and validation loss for the DNN based learning algorithms. (b) the training and validation loss of DNN16 and DNN64 are shown to be relatively the same and became stable from 40<sup>th</sup> to 60<sup>th</sup> epoch.

Given that all the models achieved very good prediction errors with the entire training set as can be observed in Figure 7, it can be stated that the models were able to accurately fit the training data very well. This is particularly true for the decision tree-based models, RFR and XGBR, that achieved the yield errors of 0.00009 t/ha and



0.000095 t/ha, respectively, followed by the DNN based models, DNNR64 and DNNR16, with yield errors of 0.0162 t/ha and 0.0172 t/ha, respectively. However, without splits to the training set, it might be difficult to fully observe the overall fit of the models to the training data. Therefore, the performance of the predictive algorithms to learn the training data was further validated using cross-validation and visualized using a violin plot as shown in Figure 8. The violin plot is a descriptive statistical tool for visualizing a given data distribution and its probability density. It can be observed in Figure 8 that the yield errors obtained from 10 splits of the training set, with replacement, exhibited different distributions and probability densities. The DNNR64 yield errors deviated from the median of the distribution with most yield errors within 0.01 t/ha and similar distribution can be observed for XGBR. The RFR yield errors showed *no variance*, though there is a high disparity (outlier) single point. On the other hand, the DNNR16 yield errors were skewed towards the interquartile range. Overall, all the predictive models yield errors are small, which demonstrates that they are a good fit to the training data.

**Fig. 8**



Visualizing distribution and probability density of training error of the predictive algorithms on the training data using violin plot. The yield errors are obtained from 10 splits of the training set with replacement for (a) DNN based learning algorithms and (b) decision tree-based learning algorithms.

### 3.2.2 Performance on Test Set with Different Evaluation Metrics

Another viewpoint of the models' performance is through performance evaluation on the test set. If the models perform as well as they performed on the training set, then the models can be designated as good models for the given regression task. Here, the RMSE, MAE, and their combined version will be used for evaluation.

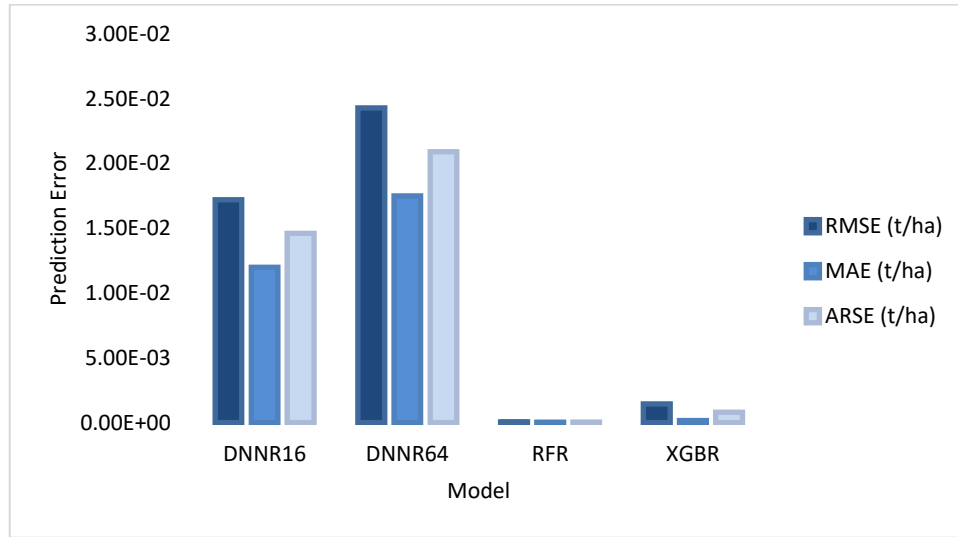
The RMSE and MAE are two popularly used metrics for evaluating the performance of regression algorithms. The outcome of using these metrics is presented in Table 2 and Figure 9 alongside the ARSE which is expected to combine the strengths of both metrics while overcoming their shortcomings. Interestingly, all the obtained

yield errors were on average less than 0.02 t/ha which reflects how well the models are good fits to the data. In the order of performance, RFR, XGBR, DNNR16, and DNNR64 models achieved yield prediction errors of approximately 0.00 t/ha, 0.00 t/ha, 0.01 t/ha, and 0.02 t/ha, respectively. The RFR and XGBR models can be observed to be the best performing models. However, their 0.00 t/ha yield errors might suggest the models are memorizing the data so perfectly well.

Table 2 Performance evaluation of the importance of feature selection in yield prediction pipeline using the test set

Mode	Model	RMSE (t/ha)	MAE (t/ha)	ARSE (t/ha)
w/o-FS	DNNR16	0.0296	0.01561	0.0139
w-FS	DNNR16	0.0172	0.01195	0.00525
w/o-FS	DNNR64	0.0296	0.01764	0.0119
w-FS	DNNR64	0.0243	0.01745	0.00685

Fig. 9



Predictive models performance across different evaluation metrics. All models achieved less than 0.02 t/ha error and ARSE is shown to give a good balance of the errors of RMSE and MAE.

The RFR and XGBR models both originated from the family of decision tree models, therefore are likely to have things in common, especially with respect to how the tree is generated. The decision tree-based models have a shortcoming, which is that they are sometimes biased towards high cardinal features. A cardinal feature contains a high number of unique numerical values that encode its various categorical entries. For instance, the state variable is a high cardinal feature because each of the 23 states are uniquely encoded. This means the state variable has the potential to cause a model to be heavily dependent on it for decision-making. Possibly, the cardinality problem can be higher and more likely when the explanatory variables are not strongly correlated to

the outcome variable. If this is the case, then the model is likely to strongly depend on the high cardinality features. These types of features can hinder a model's ability to adapt to sudden and gross changes to the explanatory variables which is likely for weather and soil data due to climate change.

In Figure 9 the RMSE errors can be observed to be higher compared to the MAE errors. This shows that there are sample points in the test set with large residual differences, which probably caused the yield error to be higher with RMSE but obscured with MAE error. However, the new metric, AARSE, can be observed to have achieved a good balance between their errors.

### 3.2.3 Generalization Capability of the Predictive Models

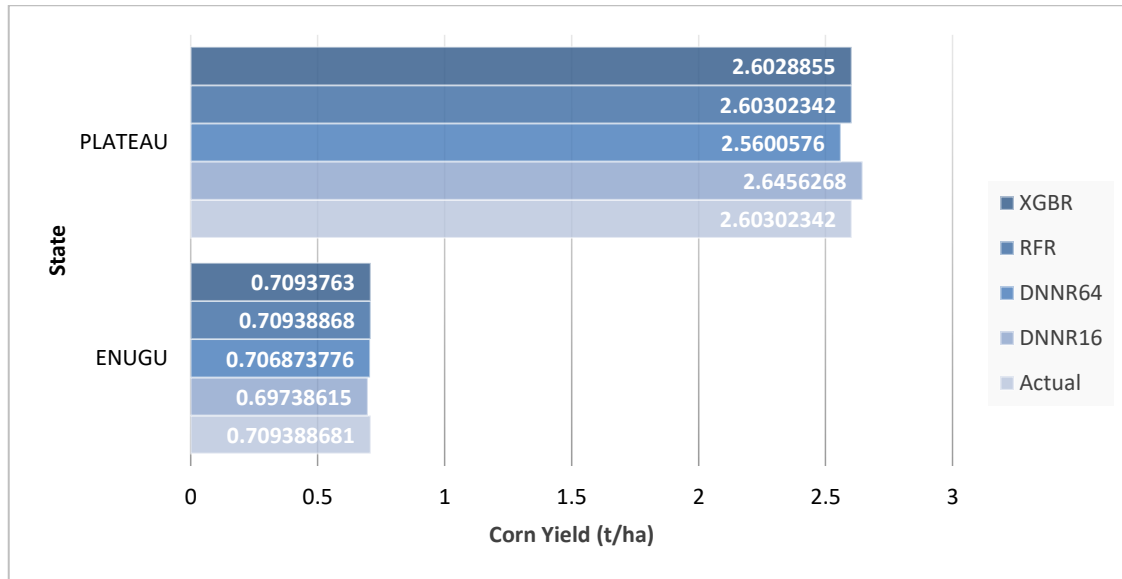
The generalizability criterion of every model must be tested before it can be deployed for use in the real world. The criterion is satisfied when a model can predict the value of an outcome variable when presented with different numeric combinations of the explanatory variables (unseen during training) and when its performance is comparable to when using the training set.

To investigate how the proposed predictive models satisfy this criterion, the same data points from the test set will be evaluated across the different predictive models. The sample data points of interest include features that describe two states, Enugu and Plateau. The Enugu state has explanatory variables and features of average minimum temperature – 21.69208848, avg-precipitation - 133.5208333, average wind speed - 1.498848967, pH - 5.466666667, sand - 59.83333333, silt - 10.16666667, and hectare - 0.545488917 which are expected to result in a yield of 0.709388681 in tonnes per hectare. Then the Plateau state has explanatory variables and features of average minimum temperature – 16.68546347 ( $C^0$ ), average-precipitation - 99.125 (mm), average wind speed - 2.417177081 ( $m\ s^{-1}$ ), pH - 5.566666667, sand - 35.5 ( $g\ 100^{-1}$ ), silt - 27.33333333 ( $g\ 100^{-1}$ ), and cultivation area - 1.686767501 hectare and expected to result in a yield of 2.60302342 in tonnes per hectare. The models were observed based on 1) generalization to unseen samples, and 2) generalization of the models to unforeseen samples. The unforeseen sample is coined in this paper to represent sudden change in values of an explanatory variable. This type of test is rarely done in literature, but it is necessary because it has strong implications for real-world use.

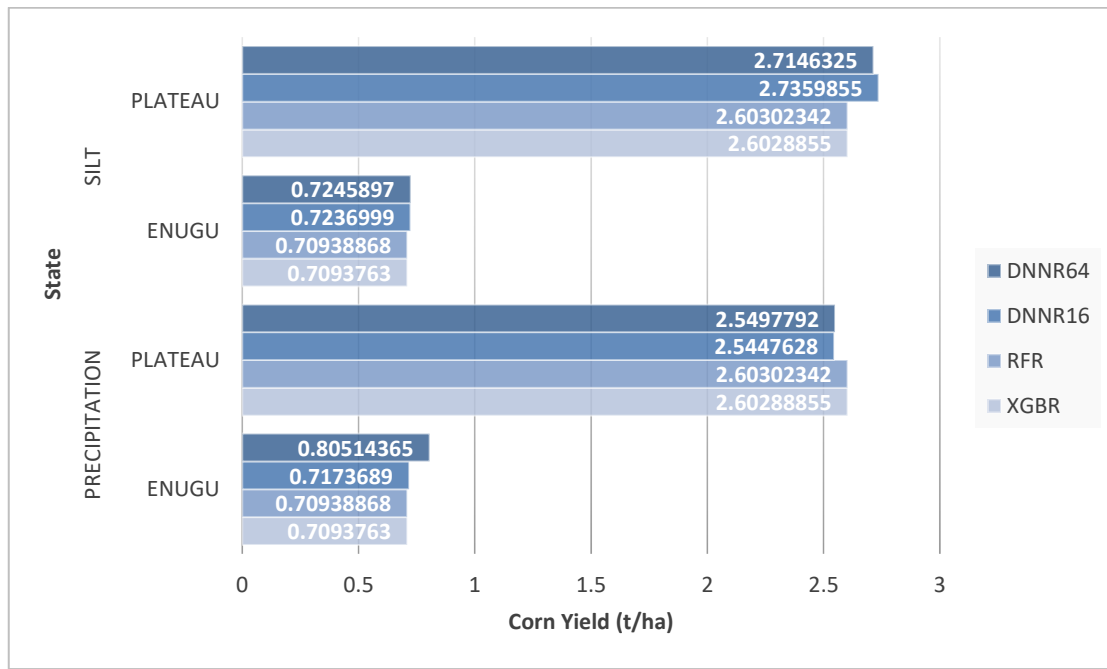
Figure 10 (a) illustrates the models' prediction errors observed based on (1) for Enugu and Plateau states. The DNN based models, DNNR16 and DDNR64, were observed to have achieved residual errors of 0.0426 t/ha and 0.0429 t/ha, respectively, while the decision tree-based models, RFR and XGBR, achieved residuals of 0 t/ha and 0.00013792 t/ha, respectively between the predicted and the actual values. The RFR and XGBR models predictions closely resemble the actual yield values, which resemble memorization and might suggest that they might be susceptible to the high cardinality features. On the other hand, the DNN models, DNNR16 and DDNR64, maintained impressive residual error differences between the predicted and the actual.

Further observations (see Figure 10 (b)) of the model's performance based on (2) were achieved by altering two explanatory variables, precipitation, and silt, individually. These variables were chosen because they exhibited strong correlation, negatively and positively, to yield. As can be observed in Figure 4, silt is expected to have more impact on yield than precipitation, among other interacting variables. This implies that on decrease of precipitation, the yield increased and vice versa, and for every change in silt, the yield is expected to increase. The precipitation for Enugu and Plateau states changed from 133.5208333 to 13.5208333, and 99.125 to 9.125, respectively, while silt changed from 10.1666667 to 27.1666667, and 27.33333333 to 50.33333333, respectively. In Figure 10 (b) it can be observed that the decision-based models, RFR and XBGR, predictions practically remained unchanged for Enugu and Plateau states despite changes in precipitation and silt. This performance further reveals that when only few explanatory variables are highly correlated to the outcome variable, the decision tree-based models might start becoming susceptible to high cardinality features. However, the DNN based models utilized some (although possibly small) of the association between the explanatory and outcome variables to build a model that generalizes well to the unforeseen changes. These are also in accordance with the expected impact of precipitation and silt to yield, as shown in Figure 4.

**Fig. 10**



(a)



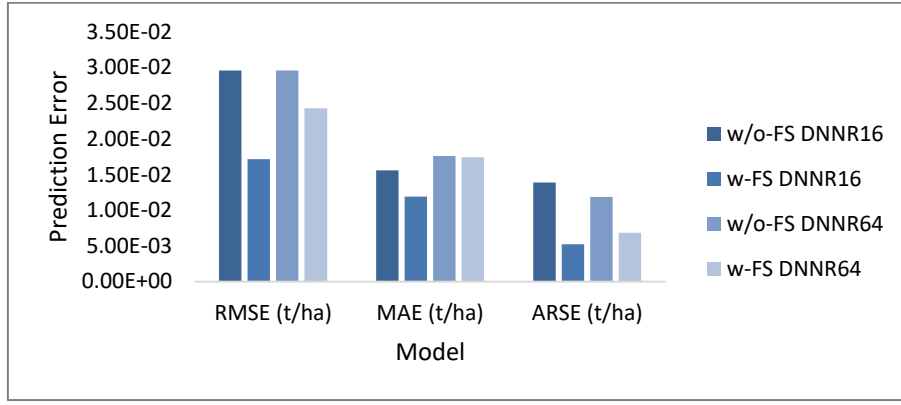
(b)

A test of generalization of the predictive models to unseen and unforeseen data points during training. The models' prediction errors on the unseen data points are plotted in (a) and for the unforeseen data points are plotted in (b). The unforeseen data points were created by increasing the values of two significant explanatory variables, precipitation, and silt, individually.

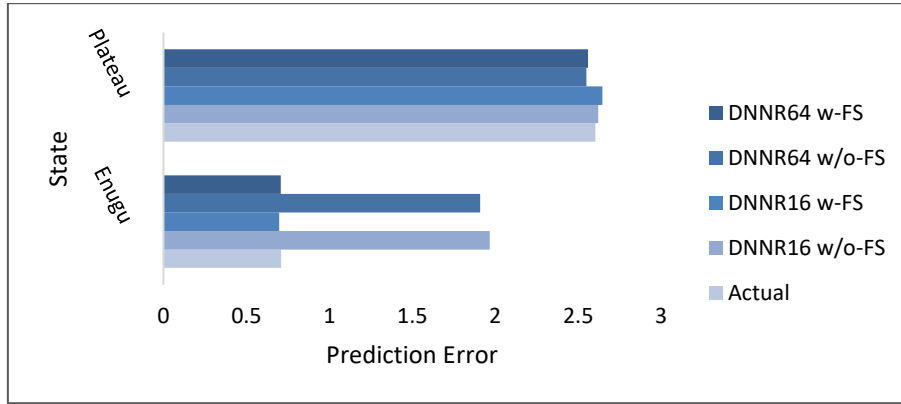
### 3.2.4 Significance of Feature Selection

Here, the aim is to observe the contribution of feature selection to performance gains of the prediction models. The experiment carried out includes generating prediction errors with the DNN based predictive models with and without feature selection. The outcome of the experiment can be visualized in Figure 11 (a), and Figure 11 (b) which captures performance on the entire test set and on two sample points, respectively. It was interesting to observe that feature selection significantly contributed to the performance gains of the predictive models in both evaluation instances shown in Figure 11 (a) and 11 (b).

**Fig. 11**



(a)



(b)

Importance of feature selection in the prediction pipeline. A capture of performance on the entire test set (a) and generalization on two datapoints (b).

In Figure 11 (a), this paper's newly defined evaluation metric for the regression task, AARSE, can be clearly seen to overcome the sensitivity and insensitivity of RMSE and MAE to outliers. A good example of insensitivity of MAE to outliers in the residual errors can be observed for the DNNR64 prediction errors recorded with and without feature selection. However, the difference in performance for both DNN based models, DNNR16 and DNNR64, became more obvious when the AARSE outcome for both models with and without feature selection were compared. The observed differences are 0.00865 t/ha and 0.00505 t/ha, respectively. The results of the importance of feature selection to the machine learning pipeline, cannot be overemphasized, as can be observed in Figure 11 (a) Categorically, feature selection does have an overall impact on the performance of the DNN models.

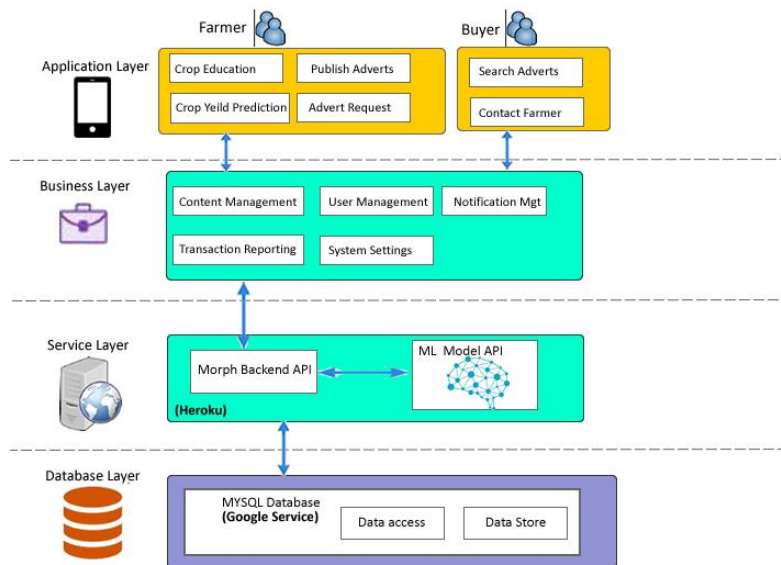
Figure 11 (b) further provides insight into how the contribution of feature selection translates to data points unseen during training. Once again, the samples from the two states, Enugu, and Plateau, at different geographical locations of Nigeria, are used. The results of applying the predictive models, DNNR16 and DNNR64, on the sample data points with and without feature selection show that that the impact of feature

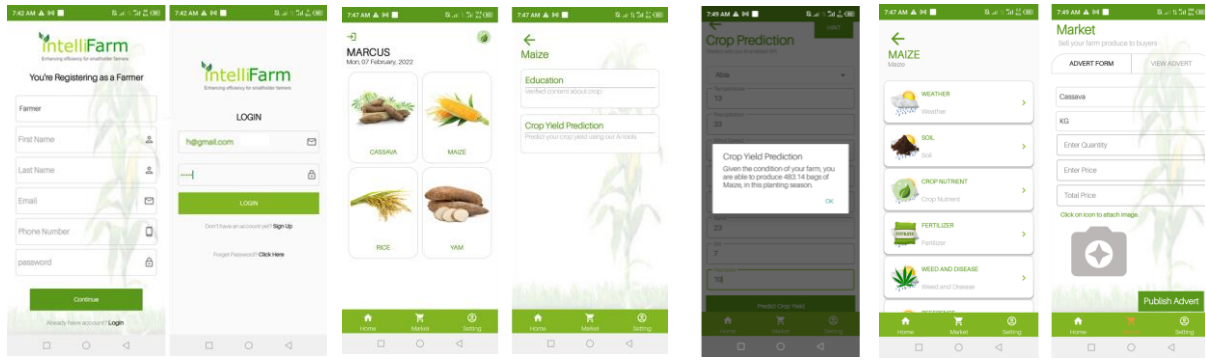
selection varies with datapoint. For the Plateau state datapoint, feature selection did not appear to impact on the prediction error recorded with and without feature selection. However, a huge difference of about 1.25 t/ha prediction errors was recorded for the DNN based models with and without feature selection.

### 3.3 Smallholder Farmer Decision Support System

The mobile phone is a technology that is commonly used in every country across the globe and, if properly utilized, can become a powerful and portable artificial intelligence (AI) tool for performing intelligent tasks. Smallholder farmers have access to mobile phones and studies [36] have shown that farmers use them for reaching out to potential buyers for their farm produce, and possibly to search the internet for answers to challenges they are posed with at the farm. This paper argues that mobile phone technology can be advanced with AI to transform the farming experience of smallholder farmers. A *proof-of-concept* mobile application was designed and developed by the authors. In this paper, it is termed “IntelliFarm” and has key functionalities of: 1) farmer-market communication module to enable farmers have direct access to buyers and vice-versa, and 2) education module which will constantly be updated with best farming practices, and 3) crop yield predictive model to help smallholder farmers make farming decisions ahead of a planting season around yield estimates based on the current states of a farm. The architecture of “IntelliFarm” is schematically shown in Figure 12 along with screenshots of the mobile application functionalities pertaining to yield prediction.

**Fig. 12**





(a)

(b)

(c)

(d)

The Decision support system mobile application architecture (upper) with four layers - the application, business, service, and database. The graphical user interface of the mobile application depicts the core functionalities (bottom). The farmer registration and login interface (a), welcome page (b), and prediction module (c), and education and market access (d).

The application architecture comprises the application layer, the business layer, the service layer, and the database layer. The application layer represents the users of the application, the farmer and the buyer who can sign up and login to access the application (see Figure 12 (a)) and perform core processes. These include sourcing for educative materials for improving soil profile, creating farm produce profiles to enable the farmer to market produce to buyers, or predicting crop yield as shown in figure 12 (b). The business layer is the backend of the application, and ensures that the user accounts, notifications, and application usage reports are generated and stored. The service layer includes the application backend currently hosted under the Heroku cloud for hosting the corn yield predictive model. It is expected that when the smallholder farmer inputs the geolocation of their farm and the numeric values of the explanatory variables, they can estimate yield, *in bags per hectare*, for a given planting season. Prediction can be activated by clicking the prediction button. This sends a hypertext transfer protocol (HTTP) application programmers' interface (API) request to the deployment environment, Heroku Cloud, where the prediction model is hosted. Once the model receives the request, it runs an inference with the data and returns the model's prediction for corn yield, to the farmer. It should be noted that the earlier deployed model in the early prototype is RFR, but any of the models can be used when the system is ready to be rolled out. The database layer is managed by the database management system, MySQL, hosted by Google Services. The data stored in the database are the farmer data, educative contents, and images of farm produce for marketing to potential buyers. To help the smallholder farmer with generating the required explanatory variables with ease, a third-party weather API can be utilized to retrieve temperature, precipitation, wind speed data in real-time, though this option was not explored in the current development. The education module is



expected to provide tips on how local materials can be sourced for measuring soil profiles. Another valuable resource provided is a user manual, designed to help the smallholder farmer navigate the application with ease.

### 3.4 Discussion

The agricultural highlight of this paper is corn yield prediction as it directly impacts the smallholder farmer. With the proposed corn yield prediction model, the smallholder farmer can be empowered to make informed decisions ahead of a planting season given weather, soil, and cultivation area. More importantly on a computational level is the designed DNNR16 and DNNR64 models with outstanding capability in corn yield prediction and versatility under several scenarios of performance: overall prediction error, metrics evaluation, and generalization to unseen and unforeseen data. Although the RFR and XGBR models achieved the lowest prediction errors, it was found that they were reliant on cardinality features, with behavior likened to memorization. This behavior became obvious through tests for generalization to unforeseen data, and since it is contrary to their performance on tabular data in the literature, we can only conclude that 1) there are small differences in the numeric values of the explanatory variables across different states, 2) there is a non-linear relationship between the explanatory variables and the outcome variables, 3) there is a weak correlation, in most cases, between the explanatory variables and the outcome variables. Point (1) might have forced the decision tree-based models to depend on high cardinality features for variance across data points. Although the RFR and XGBR models achieved the smallest prediction errors both with the RMSE and MAE metrics for each of the sample data points evaluated, they could not accommodate any sort of changes to two of weather and soil, precipitation, and silt variables, which among other variables were identified via feature selection to show interaction with yield. The latter is strongly positively correlated while the former is strongly negatively correlated. It was observed that when precipitation value was reduced and silt value was increased, yield increased and vice-versa. Although the degree of decrease or increase was not quantified in this paper because changes in the values could potentially take any form due to the dynamic nature of weather and soil due to climate change. However, these observations were made with the DNNR16 and DNNR64 models. They showed superiority over the decision-based models for the regression task. On the other hand, the RFR and XGBR prediction errors remained unchanged despite changes to the values of these variables. Additionally, a new regression metric, AARSE, has shown that the integral of RMSE and MAE can overcome their shortcomings related to outlier sensitivity (RMSE) and outlier insensitivity (MAE). This metric can be explored by other researchers, looking for that metric which provides the right balance of prediction errors.

While there is no direct basis of comparison of this study to existing works [11]-[17] because different geolocations impose different impacts on crop farming, the correspondence and similarity between them is worth noting. This pertains to the weather and soil variables that interacted with yield. It is a known fact that neural networks are not great at quantifying the contributions of explanatory variables to outcome variables. However, this study took a different approach of working out the features most significant through a feature selection

method and using that subset as the representative features for the neural network. Therefore, these features will serve as the basis of comparison to existing literature. For the weather variables, the minimum temperature was identified in [14] to be more correlated to yield than other temperature variables, such as the maximum and average temperatures. This finding corresponds with the observation of this study. As shown in Figure 4, the Kendall correlation coefficient indicates that minimum temperature contributed more to yield than maximum and average temperature. However, it ranks as a weakly correlated feature for all identified correlated features such as: hectare (cultivation area), silt, average precipitation, sand, soil pH, and wind speed. Note that these variables are arranged in the order of importance. The contribution of precipitation to yield was validated in this study and is confirmed in [14] and [12] to be significantly linked to yield. The soil variables on the other hand showed great variability across literature. However, it was interesting to observe that silt and sand components of the soil profile (which were found in this study to be correlated to yield) coincide with the empirical results on the impact of soil analysis in agronomy. An example is [37] where the highest corn yield was obtained in sandy loam soil. The latter is a soil type formed from the combination of silt and sand soil.

Other considerations of empowerment of the smallholder farmer that the decision support system provides are: enabling the smallholder farmer to have a direct access to market thereby eliminating third party or middleman involvement in farmer's farm-to-market communication, and provision of educational resources to help the smallholder farm be well-equipped to tackle farming challenges related to corn yield, fertilization, irrigation and other maintenance practices through educational resources. For instance, let's assume that the smallholder farmer, through a yield estimate with the prediction model, decides that a predicted yield is below his/her expectation for a given planting season. Here the educational resources can be used by the farmer to gain insight into possible factors the farmer can control, such as soil pH, silt and sand content of soil, to ensure that expected yield can be achieved when interacting with weather factors which the smallholder farmer is unable to control. We have so far discussed the underlying strengths of this paper, but there are several improvements to the methodology that can necessitate future research. This study was limited to the modelling of only variables that the smallholder can easily acquire using available local resources in the farm for soil data, or third-party APIs for weather data in real-time. However, other variables such as organic radiation, water vapour, or saturated volumetric water content, might be relevant to yield and might be easily resourced by much large-scale farms and can therefore be included in features considered in the preprocessing step. Also, only corn yield was considered in this study, whereas there are other staple foods such as yam, cassava, guinea corn, and rice, with varying requirements for weather and soil interactions, that can be incorporated through use of additional data and further modelling.

#### **4 Conclusion**

This paper proposed a deep neural network regressor (DNNR) model where the depth and number of neurons of the hidden layer, amongst other hyperparameters, were defined to enable the network to learn to model the

non-linear complex interaction between soil and weather data accurately. A new metric, AARSE, which combines the strengths of RMSE and MAE, was proposed for the regression task, and it forms a balance between RMSE which is sensitive to an outlier, and MAE which is insensitive to an outlier. With AARSE, the RFR, XGBR, DNNR16, and DNNR64 achieved yield prediction errors of 0.0000294 t/ha, 0.000792 t/ha, 0.0146 t/ha, and 0.0209 t/ha, respectively. However, when generalizability to unforeseen data due to changes to values of some of the explanatory variables was carried out, the DNNR models exhibited better modelling of the non-linear complexities of the environmental variables relative to their real-world agricultural expectations. The RFR and XGBR behaviors in such scenarios demonstrated their susceptibility to high cardinality problems. Further analysis revealed that a strong interaction existed between weather and soil variables, particularly with precipitation and silt variables which were shown to be strong-negatively and strong-positively correlated with yield, when precipitation value was reduced and silt value increased, yield increased and vice-versa. Although the degree of decrease or increase was not quantified in this study. Another highlight of the paper was the perspective for which the proposed yield predictive models were designed. They were fashioned to help the smallholder farmer make effective farming decisions which might have a wider and much more direct impact on alleviating food crises, in addition to the global purpose of monitoring food security and creating agricultural policies. Further advances were the design of a decision support system in the form of a mobile application. It integrated the proposed model and included educative and farmer-to-market access modules, to enable the smallholder farmer to farm smartly and intelligently. Future work centers around consolidating models for yield prediction of Africa's staple food.

## **Declarations**

### **- Funding**

This research was funded by the Global Challenges Research Fund (GCRF) (UKRI and BBSRC) with grant number 6414884 and titled "Artificial Intelligence (AI) Enhanced Smallholder Farm Software Tool".

### **- Conflicts of interest**

The authors declare that there is no conflict of interest.

### **- Ethics approval**

Not applicable.

### **- Consent to Participate**

Not applicable.

### **- Consent for publication**

Not applicable

### **- Data Availability**

The dataset analyzed has been submitted to the UCI Machine learning repository <https://archive.ics.uci.edu/dataset/843/crop+yield+prediction+with+real+weather+and+soil+data> for reproducibility.

- Code Availability

Access to the custom code is temporarily made available as a supplementary file but will be made publicly available on Github upon acceptance.

## References

1. Lowder, S.K., Skoet, J. and Singh, S., 2014. What do we really know about the number and distribution of farms and family farms in the world? Background paper for The State of Food and Agriculture 2014.
2. Lutz Goedde, Amandla Ooko-Ombaka, and Gillian Pais. Private-sector companies can find practical solutions to enter and grow in Africa's agricultural market. <https://www.mckinsey.com/industries/agriculture/our-insights/winning-in-africas-agricultural-market> [Accessed 29 01 2022]
3. Fan, S. and Rue, C., 2020. The role of smallholder farms in a changing world. In *The Role of Smallholder Farms in Food and Nutrition Security* (pp. 13-28). Springer, Cham. [https://doi.org/10.1007/978-3-030-42148-9\\_2](https://doi.org/10.1007/978-3-030-42148-9_2).
4. Meroni, M., Waldner, F., Seguíni, L., Kerdiles, H. and Rembold, F., 2021. Yield forecasting with machine learning and small data: What gains for grains? *Agricultural and Forest Meteorology*, 308, p.108555. <https://doi.org/10.1016/j.agrformet.2021.108555>.
5. Amare, M., Cissé, J.D., Jensen, N.D. and Shiferaw, B., 2017. The Impact of Agricultural Productivity on Welfare Growth of Farm Households in Nigeria: A Panel Data Analysis. FAO. Rome. <https://api.semanticscholar.org/CorpusID:167211687>.
6. Rose, D.C., Lyon, J., de Boon, A., Hanheide, M. and Pearson, S., 2021. Responsible development of autonomous robotics in agriculture. *Nature Food*, 2(5), pp.306-309. <https://doi.org/10.1038/s43016-021-00287-9>.
7. Kulbacki, M., Segen, J., Knieć, W., Klempous, R., Kluwak, K., Nikodem, J., Kulbacka, J. and Serester, A., 2018, June. Survey of drones for agriculture automation from planting to harvest. In *2018 IEEE 22nd International Conference on Intelligent Engineering Systems (INES)* (pp. 000353-000358). DOI: 10.1109/INES.2018.8523943.
8. Sushanth, G. and Sujatha, S., 2018, March. IOT based smart agriculture system. In *2018 International Conference on Wireless Communications, Signal Processing and Networking (WiSPNET)* (pp. 1-4). IEEE. DOI: 10.1109/WiSPNET.2018.8538702.

9. Shook, J., Gangopadhyay, T., Wu, L., Ganapathysubramanian, B., Sarkar, S. and Singh, A.K., 2021. Crop yield prediction integrating genotype and weather variables using deep learning. *Plos one*, 16(6), p.e0252402. DOI: 10.1371/journal.pone.0252402
10. Shahhosseini, M., Martinez-Feria, R.A., Hu, G. and Archontoulis, S.V., 2019. Maize yield and nitrate loss prediction with machine learning algorithms. *Environmental Research Letters*, 14(12), p.124026. DOI 10.1088/1748-9326/ab5268.
11. Jeong, J.H., Resop, J.P., Mueller, N.D., Fleisher, D.H., Yun, K., Butler, E.E., Timlin, D.J., Shim, K.M., Gerber, J.S., Reddy, V.R. and Kim, S.H., 2016. Random forests for global and regional crop yield predictions. *PLoS One*, 11(6), p.e0156571. DOI: 10.1371/journal.pone.0156571.
12. Alhnaity, B., Pearson, S., Leontidis, G. and Kollias, S., 2019, June. Using deep learning to predict plant growth and yield in greenhouse environments. In *International Symposium on Advanced Technologies and Management for Innovative Greenhouses: GreenSys2019* 1296 (pp. 425-432). DOI: 10.17660/ActaHortic.2020.1296.55.
13. Khaki, S., Wang, L. and Archontoulis, S.V., 2020. A cnn-rnn framework for crop yield prediction. *Frontiers in Plant Science*, 10, p.1750. <https://doi.org/10.3389/fpls.2019.01750>.
14. Ansarifar, J., Wang, L. and Archontoulis, S.V., 2021. An interaction regression model for crop yield prediction. *Scientific reports*, 11(1), pp.1-14. <https://doi.org/10.1038/s41598-021-97221-7>.
15. Shahhosseini, M., Hu, G., Khaki, S. and Archontoulis, S.V., 2021. Corn yield prediction with ensemble CNN-DNN. *Frontiers in plant science*, 12. <https://doi.org/10.3389/fpls.2021.709008>.
16. Shahhosseini, M., Hu, G. and Archontoulis, S.V., 2020. Forecasting corn yield with machine learning ensembles. *Frontiers in Plant Science*, 11, p.1120. <https://doi.org/10.3389/fpls.2020.01120>.
17. Pugnaire, F.I., Morillo, J.A., Peñuelas, J., Reich, P.B., Bardgett, R.D., Gaxiola, A., Wardle, D.A. and Van Der Putten, W.H., 2019. Climate change effects on plant-soil feedbacks and consequences for biodiversity and functioning of terrestrial ecosystems. *Science advances*, 5(11), p.eaaz1834. DOI: 10.1126/sciadv.aaz1834.
18. Olisah, C., Smith, L. N., & Smith, M. L. (2022, July). Maize yield predictive models and mobile-based decision support system for smallholder farmers in Africa. Paper presented at 17th International Conference on Machine Learning and Data Mining MLDM 2022, New York, USA. [Accessed November 8, 2022].
19. Doris D. S. Households participating in agricultural activities in Nigeria 2019, by type and area <https://www.statista.com/statistics/1119593/households-participating-in-agricultural-activities-in-nigeria-by-type-and-area/> [Accessed January 12, 2022].
20. Global climate and weather data available at <https://www.worldclim.org/data/index.html> [accessed November 10, 2020].
21. The maize production in Nigeria, available at <https://knoema.com/data/nigeria+agriculture-indicators-production+maize?unit=> [accessed January 10, 2021].

22. Soil property maps of Africa at 250 m resolution available at <https://www.isric.org/projects/soil-property-maps-africa-250-m-resolution> [accessed December 17, 2020].
23. Newbold, P., 1983. ARIMA model building and the time series analysis approach to forecasting. *J. Forecast.* 2, 23–35. doi: 10.1002/for.3980020104
24. Neina, D., 2019. The role of soil pH in plant nutrition and soil remediation. *Applied and Environmental Soil Science*, 2019. <https://doi.org/10.1155/2019/5794869>.
25. Letey, J.O.H.N., 1958. Relationship between soil physical properties and crop production. In *Advances in soil science* (pp. 277-294). Springer, New York, NY. [https://doi.org/10.1007/978-1-4612-5046-3\\_8](https://doi.org/10.1007/978-1-4612-5046-3_8).
26. Ray, D.K., Gerber, J.S., MacDonald, G.K. and West, P.C., 2015. Climate variation explains a third of global crop yield variability. *Nature communications*, 6(1), pp.1-9. DOI: 10.1038/ncomms6989.
27. Dickey, D. A., and Fuller, W. A., 1981. Likelihood ratio statistics for autoregressive time series with a unit root. *Econometrica* 49, 1057–1072. DOI: 10.2307/1912517
28. Kendall, M. G., 1938. A new measure of rank correlation. *Biometrika*, 30, 81-93. <https://doi.org/10.2307/2332226>.
29. Brophy, A.L., 1986. An algorithm and program for calculation of Kendall's rank correlation coefficient. *Behavior Research Methods, Instruments & Computers*.
30. A.S. Miller, B.H. Blott. Review of neural network applications in medical imaging and signal processing. *Med. Biol. Eng. Comput.*, 30 (5) (1992), pp. 449-464. <https://doi.org/10.1007/BF02457822>.
31. Olisah, C. C., Smith, L., and Smith, M., 2022. Diabetes mellitus prediction and diagnosis from a data preprocessing and machine learning perspective. *Computer Methods and Programs in Biomedicine*, 220, 106773. DOI: 10.1016/j.cmpb.2022.106773.
32. Agarap, A.F., 2018. Deep learning using rectified linear units (relu). *arXiv preprint*. <https://doi.org/10.48550/arXiv.1803.08375>
33. Chen, T. and Guestrin, C., 2016. Xgboost: A scalable tree boosting system. In *Proceedings of the 22nd ACM SIGKDD international conference on knowledge discovery and data mining* (pp. 785-794). Xgboost: A scalable tree boosting system
34. Friedman, J.H., 2001. Greedy function approximation: a gradient boosting machine. *Annals of statistics*, pp.1189-1232. <https://www.jstor.org/stable/2699986>.
35. Breiman, L., 2001. Random Forests. *Machine Learning* 45, 5–32. <https://doi.org/10.1023/A:1010933404324>.
36. Aker, J.C., 2011. Dial “A” for agriculture: a review of information and communication technologies for agricultural extension in developing countries. *Agricultural economics*, 42(6), pp.631-647. <https://doi.org/10.1111/j.1574-0862.2011.00545.x>.
37. Fang, J., and Su, Y., 2019. Effects of soils and irrigation volume on maize yield, irrigation water productivity, and nitrogen uptake. *Scientific reports*, 9(1), 1-11. <https://doi.org/10.1038/s41598-019-41447-z>.